Acta Crystallographica Section D
Biological Crystallography
ISSN 0907-4449

Crystallization of diaminopimelate decarboxylase from *Escherichia coli*, a stereospecific D-amino-acid decarboxylase

Cory Momany,* Vladimir Levdikov, Lena Blagova and Kristine Crews

Department of Pharmaceutical and Biomedical Sciences, Wilson College of Pharmacy, University of Georgia, Athens, Georgia, USA

Correspondence e-mail: cmomany@mail.rx.uga.edu

Received 14 September 2001
Accepted 2 January 2002

The final step in lysine biosynthesis in bacteria, the conversion of *meso*-diaminopimelate to L-lysine, is catalyzed by the only known D-amino-acid decarboxylase, diaminopimelate decarboxylase (DDC). The *Escherichia coli* DDC has been cloned, overexpressed in *E. coli* with a carboxy-terminal polyhistidine purification tag and crystallized from lithium sulfate. The protein is intensely yellow, owing to the pyridoxal-5′-phosphate cofactor, and is enzymatically active. Large well ordered crystals, belonging to space group $P6_122$ with unit-cell parameters $a = b = 98.6$, $c = 177$ Å, make high-resolution X-ray diffraction studies possible to characterize the residues important in stereospecific decarboxylation and reprotonation during catalytic turnover.

1. Introduction

Diaminopimelate decarboxylase (DDC; encoded by the *lysA* gene) is responsible for the final step in the stereospecific synthesis of L-lysine by microorganisms.

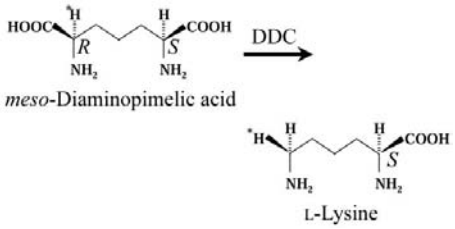

Lysine biosynthesis in bacteria occurs *via* a series of highly regulated reactions from aspartic semialdehyde (Cohen, 1985). Two products in the pathway are necessary for growth: *meso*-diaminopimelate (DAP) and L-lysine. While lysine is principally utilized in protein synthesis, DAP is a cell-wall component that cross-links peptidoglycan polymers in most bacteria, excluding some Gram-positive cocci which use lysine. Cessation of lysine synthesis by mutations in the genes or inhibition of the enzymes ultimately results in cell lysis and thus death (Patte, 1996). While DDC is a potential target for antibacterial therapy (Girodeau *et al.*, 1986), no effective inhibitors with inhibition constants in the submicromolar range or better have been identified using standard synthetic approaches. An atomic structure could provide some direction for the design of more potent inhibitors.

DDC is a pyridoxal-5′-phosphate (PLP; vitamin B_6) dependent decarboxylase with a monomeric molecular weight of 46 099 Da consisting of 420 amino acids (Stragier *et al.*, 1983). The purified enzyme isolated from *E. coli* has a predicted apparent molecular weight of ∼200 kDa as determined from ultracentrifugation studies, with maximal activity at pH 6.8 (White & Kelley, 1965). A polyhistidine-tagged *E. coli* DDC has been previously overexpressed that appears to be monomeric (Bourot *et al.*, 2000) by gel-filtration analysis.

DDC has substantial sequence similarity to eukaryotic ornithine decarboxylases and as such belongs to the alanine racemase structural group (Grishin *et al.*, 1995). The structures of a mouse ODC (mODC; Kern *et al.*, 1999) and the *Typanosoma bruceii bruceii* ODC (TbODC) with and without difluoromethylornithine (DFMO) have been reported (Grishin *et al.*, 1996, 1999) as well as a mutant structure (Jackson *et al.*, 2000). Unlike the eukaryotic ODCs, which decarboxylate L-ornithine, DDC decarboxylates a substrate having both L- and D-amino-acid chiral centers, *meso*-diaminopimelic acid. The stereospecificity of DDCs toward DAP results in inversion of the chiral center (Asada *et al.*, 1981) and inversion may occur with the eukaryotic ODCs. This is in contrast to other bacterial decarboxylases, such as the bacterial ODC, glutamate and histidine decarboxylases, where retention of configuration is conserved (Abell & O'Leary, 1988; Asada *et al.*, 1984;

© 2002 International Union of Crystallography
Printed in Denmark – all rights reserved

Yamada & O'Leary, 1978). Here, we report the crystallization of a polyhistidine-tagged DDC from *E. coli*.

2. Methods

2.1. Cloning, overexpression and purification of DDC

A vector containing the DDC protein coding sequence with a C-terminal polyhistidine purification tag was created using the strategy from the Seamless Cloning Kit (Stratagene). DNA encoding DDC was generated by PCR amplification using *Pfu* polymerase with the vector pLC3-8 (obtained from the *E. coli* Genetic Stock Center at Yale University) as template. The PCR primers contained *Eam*1104 restriction sites (*Eam*1104 is a critical component of the Seamless Cloning Kit; it recognizes non-methylated DNA with the sequence 5′-CTCTTC-3′ and cuts 1 and 3 bases from the 3′-end of this recognition sequence) and the 5′ and 3′ coding sequences of DDC (forward primer 5′-CG*CTCTTC*T**ATG-**CCACATTCACTGTTCAGC-3′ with the *Eam*1104 site in italics and the initiating codon in bold; the reverse primer 5′-GC*CTCTTC*G**GTG**AAGCAATTCCA-GCGCCAGTAATTC-3′ with the *Eam*1104 site in italics and the anticodon encoding a histidine in the polyhistidine purification tag). The resulting PCR product was cloned into pET28b vector (Novagen), similarly amplified with *Eam*1104 restriction sites (forward primer 5′-GC*CTCTTC*C**CAC**CA-TCATCATCATCACTGAAGCGGCCTG-3′ with the *Eam*1104 site in italics and the first histidine of the tag in bold; reverse primer 5′-CG*CTCTTC*C**CAT**GGTATAT-ctccttcTTAAAGTTAAAC-3′ with the start anticodon in bold and the Shine–Dalgarno site of the vector in lower case) producing the construct pCM1. The design strategy included using the first polyhistidine tag already present in the pET28b vector, which is usually used for creating N-terminal tags. A stop codon was also added. This strategy maintained a majority of the restriction sites within the pET28b vector's multiple cloning site. The first three nucleotide bases, 5′-CAT-3′, in the pET28b polyhistidine tag were mutated to 5′-CAC-3′ so that force cloning was possible. If the sequence CAT was used, the PCR insert would have ligated in a random orientation after cutting with *Eam*1104 since the resulting overhang would be complementary to the ATG on the other end of the insert. The resulting protein encoded on the plasmid thus contained a hexahistidine-tag at the C-terminus of the protein for ease of purification. Attempts to clone DDC into T7-based vectors that did not contain the gene for lactose repressor were never successful. The plasmid pCM1 was transformed into either XL-I blue cells for characterization and sequencing or into BL21(DE3) for high-level expression.

Table 1
Data-collection statistics.

Values in parentheses refer to the highest resolution shell.

Wavelength (Å)	1.54178
Space group	$P6_122$
Unit-cell parameters (Å)	$a = b = 98.66$, $c = 177.07$
No. of observed reflections	304753
No. of unique reflections	29807
Resolution range (Å)	20.0–2.1 (2.12–2.10)
Completeness (%)	98.0 (73.1)
$I/\sigma(I)$	27.8 (4.1)
$R_{\rm merge}$(%)	6.8 (20.6)

A 50 ml culture of *E. coli* strain BL21(DE3) transformed with pCM1 was grown for 15–17 h at 310 K in a LB medium containing 50 µg ml^{-1} kanamycin and 0.1 m*M meso*-diaminopimelate from a single colony. After inoculation into 1 l of the same medium, the cells were grown for 4–5 h and then induced with 1 m*M* IPTG (isopropyl-β-D-thiogalactoside) for 4 h. The cells were collected by centrifugation at 277 K for 15 min at 10 000*g* and suspended in 30 ml extraction buffer (0.02 *M* sodium phosphate, 0.5 *M* NaCl, 0.2 m*M* pyridoxal-5′-phosphate pH 7.4) and either used immediately or frozen at 253 K for later use. The cell suspension was cooled in ice to 283 K and sonicated for 3 min in 1 min increments with a Fisher Scientific 550 sonic dismembrator set at 50% duty cycle while maintaining the temperature below 288 K. Cellular debris was removed by centrifugation for 20 min at 25 000*g* at 277 K followed by centrifugation at 60 000*g* for 20 min. The clear supernatant was applied to a Pharmacia Hi-Trap Chelating 5 ml column charged with Ni^{2+} (using 0.2 *M* nickel sulfate) that had been equilibrated with 20 m*M* sodium phosphate, 0.5 *M* NaCl pH 7.4 at a rate of 2 ml min^{-1} following Pharmacia's recommended procedure. The enzyme was washed with the same buffer and then eluted with a linear gradient of imidazole (0–0.5 *M* over 20 column volumes) pH 7.4 in the same buffer. All chromatography was performed at room temperature using a Pharmacia ÄKTA purifier. The fractions containing DDC were combined and twice concentrated to 5 ml by ultrafiltration (YM10 membrane, Amicon) and diluted to 50 ml with 50 m*M* MES buffer pH 6.0 containing 0.2 m*M* PLP or dialyzed into buffer. The resulting solution was applied to a 5 ml Pharmacia HiTrap S column pre-equilibrated with 50 m*M* MES pH 6.0 lacking PLP at a rate of 2 ml min^{-1} (buffer *S*). The enzyme was washed with the same buffer and then eluted using a linear gradient of 0–0.5 *M* NaCl in buffer *S* over 20 column volumes. The brightly yellow fractions containing DDC were combined and dialyzed against 50 m*M* MES buffer pH 6.0 containing 0.2 m*M* PLP. For crystallization trials, the protein was concentrated to 20–30 mg ml^{-1} using Ultrafree 4 Biomax 10 ultrafiltration concentrators.

2.2. DDC enzyme assay

DDC enzymatic activity was initially confirmed by an enzyme-coupled assay (Scriven *et al.*, 1988) and then more carefully determined using a ninhydrin-based colorimetric method (Work, 1957). For the enzyme-coupled assay, DDC (10 µl) was added to 2 ml of 10 m*M meso*-DAP dissolved in Sigma Infinity Reagent (Sigma Co.). The change from NADH to NAD^+ was spectrophotometrically monitored at 360 nm at room temperature or 310 K. Carbonate standards (Sigma) were used to calibrate the system. An accurate optimal specific activity cannot be directly determined from this assay because there is a delay in the conversion of carbon dioxide to carbonate, which is measured indirectly though an absorbance change as carbonate is converted to oxaloacetate using phophoenolpyruvate carboxylase with the oxaloacetate and then reduced using NADH and malate dehydrogenase. A more accurate enzyme-determination monitored the conversion of diaminopimelate directly through a colorimetric ninhydrin-based assay (Work, 1957). Each ninhydrin assay reaction consisted of 0.1–1.0 ml enzyme, 0.25 ml 10 m*M* β-mercaptoethanol, 10 µg PLP, 0.4 ml 5 mg ml^{-1} *meso*-DAP and 100 m*M* sodium phosphate pH 6.8 in a total reaction volume of 2.5 ml. Samples were incubated with shaking at 310 K and 0.1 ml aliquots were removed every 5 min and added to 4 ml acetic acid, 0.4 ml H_2O and 0.5 ml ninhydrin reagent (250 mg ninhydrin dissolved in a mixture of 4 ml 0.6 *M* phosphoric acid and 6 ml acetic acid). After heating the ninhydrin-treated samples at 310 K for 90 min, the absorbance at 440 nm was recorded and compared with a standard curve prepared using L-lysine and *meso*-diaminopimelate.

2.3. Gel-filtration analysis of DDC

The molecular weight of the DDC was determined by gel filtration on a Sephacryl

Figure 1
Photograph of a cluster of DDC crystals. The yellow colour arises from the presence of the pyridoxal-5′-phosphate cofactor.

S-300 high-resolution column (26 × 60 cm) (Pharmacia Biotech). Calibration was performed with the following protein standards: thyroglobulin (669 kDa), apoferritin (443 kDa), β-amylase (200 kDa), alcohol dehydrogenase (150 kDa), albumin (66 kDa) and carbonic anhydrase (20 kDa). A sample of the post-S column DDC (0.5 ml at 2 mg ml^{-1}) was eluted through a column equilibrated with 50 m*M* sodium MES pH 6.0 at a flow rate of 1 ml min^{-1}.

2.4. Crystallization and X-ray analysis

Initial conditions for crystallization of DDC were identified in sparse-matrix screens (Jancarik & Kim, 1991) with Hampton Research crystallization kits (Crystal Screens 1 and 2) using the vapour-diffusion method (McPherson, 1976) at room temperature. For initial screens, DDC was dialyzed into 20 m*M* Tris–HCl, 0.2 m*M* PLP pH 8.0. Crystallization conditions at neutral pH values (pH 5–8) with 1 *M* ammonium sulfate were successful. For further optimization of these conditions, lithium sulfate was used as the primary precipitant because heavy-atom preparation would be more successful with lithium ions than with ammonium ions; the ammonium ions can also interfere with the binding of the PLP cofactor, with a concomitant loss of activity. Crystals suitable for final high-resolution data collection were grown from 2 µl native protein sample (at a concentration of 15–20 OD_{280} in 50 m*M* sodium MES buffer pH 6.0, 0.1 m*M* PLP) mixed with 2 µl well solution (1.44–1.54 *M* lithium sulfate as a precipitant; 50 m*M* MES buffer pH 6.0, 0.1 m*M* PLP) suspended on plastic cover slips over 1.0 ml well solution in Linbro plate wells. A stabilizing solution (2.5 *M* Li_2SO_4, 0.2 m*M* PLP, 0.1 *M* MES buffer pH 6.0) is useful for heavy-atom preparation. For the native data collection reported here, crystals were briefly transferred through a cryoprotectant solution containing 2.5 *M* Li_2SO_4 (or saturated Li_2SO_4), 15–20% 2,3-butanediol, 3 m*M* PLP, 0.1 *M* MES buffer pH 6.0. Native data from a single flash-frozen crystal were collected on an MAR scanner mounted on a Rigaku RU-200 rotating-anode generator operated at 100 kV and 50 mA producing Cu $K\alpha$ radiation. Each frame was exposed for 600 s with a 0.5° oscillation at crystal-to-detector distances of 200 and 250 mm and then processed with the *HKL* package (Otwinowski & Minor, 1997).

3. Results

3.1. Protein characterization

Approximately 20–30 mg of purified polyhistidine-tagged DDC can be obtained from a 1 l culture (5 g wet weight). DDC was homogeneous (>95% pure) by SDS–PAGE (Pharmacia PHAST system), but showed two major species (not further characterized) on IEF and native PAGE analysis. The purified protein has the clear characteristic of a PLP-dependent protein, a yellow color with an absorption maximum around 426 nm. The metal-chelate column step alone produces a relatively homogeneous protein, but the cation-exchange column removes some minor contaminants. The specific activity of the purified DDC was 7 µmol min^{-1} mg^{-1} at 310 K using the ninhydrin-based assay in 100 m*M* sodium phosphate buffer pH 6.8. This value agrees fairly well with the 9 µmol min^{-1} mg^{-1} specific activity reported for DDC purified directly from *E. coli* (no His tag; White & Kelley, 1965) using the same assay. The lower specific activity compared with the wild-type DDC is explained by our use of β-mercaptoethanol (BME) instead of the 2,3-dimercaptopropan-1-ol (BAL) used by White and Kelley. DDC was reported to have 43% of the activity in BME compared with BAL (White & Kelley, 1965). However, our specific activity is tenfold lower than that reported by Bourot *et al.* (2000), 77 µmol min^{-1} mg^{-1}, for their polyhistidine-tagged *E. coli* DDC, where a different assay system was utilized. The difference is likely to arise from the assay system, but at this time no analysis of the differences has been made. The specific activity of our DDC was 4.1 µmol min^{-1} mg^{-1} in 50 m*M* MES pH 6.0, consistent with the pH profile reported by White & Kelley (1965).

When the Ve/Vo is plotted against log molecular weight, the DDC elutes in a gel-filtration analysis as a monomer with a derived M_r of 52 500. While this is consistent with the solution species reported elsewhere for recombinant His-tagged DDC (Bourot *et al.*, 2000) and also observed using dynamic light scattering with old samples of our DDC (data not shown), it is a surprising result since the active site of the eukaryotic ODCs sits at the interface of two monomers related by a twofold. Thus one would expect DDC to be at least a dimer in solution when active. Ultracentrifugation studies indicated that wild-type DDC has a M_r of 200 000 (White & Kelley, 1965). The contradictory results may be a function of the pH used for the analyses, but as noted above our enzyme is still significantly active in MES pH 6.0. Perhaps most significant is that reducing agents were omitted from our purification protocols and were not included in the gel-filtration analysis. It seems feasible that the oxidation state of the enzyme may critically determine the oligomerization state, with reducing agents protecting functional groups necessary for formation of higher order states. DDC's absolutely conserved Cys342 is equivalent to Cys360 in TbODC, which sits next to the cofactor in the TbODC structure and is donated from a twofold-related monomer (relative to the monomer having the lysine with which the PLP is associated *via* a Schiff base). This cysteine may be sensitive to oxidation and thus block oligomerization. Alternatively, Rosner showed that the enzyme activity of the *Bacillus subtilus* DDC has a strong dependence on ionic strength (Rosner, 1975). The gel-filtration analyses reported here and by Bourot *et al.* (2000) were conducted in somewhat low ionic strength buffers. Clarification of this issue is clearly required and is in progress. The solutions used to successfully crystallize DDC contained lithium sulfate at a high ionic strength. Further, the space-group analysis described below supports the presence of oligomers having twofold relationships, which can thus generate active sites containing residues from two monomers as in the ODCs.

3.2. Crystallization and X-ray analysis

DDC crystallizes as intensely yellow hexagonal rods (Fig. 1). Crystals grow up to 1.0 mm in length in 3–4 d. Data processing of area-detector data are consistent with a hexagonal space group having 6/*mmm* Laue symmetry, with unit-cell parameters $a = b = 98.66$, $c = 177.07$ Å (Table 1). Very strong 00*l* reflections where $l = 6n$ made the data most consistent with space groups $P6_122$ or $P6_522$. However, a large number of systematic absences for $P6_{1/5}22$ with $I > 3\sigma(I)$ made the interpretation based on processed data alone somewhat ambiguous. Heavy-

atom sites identified using *SOLVE* (Terwilliger & Berendzen, 1999; data not shown) were internally most consistent and had the highest figures of merit in space group $P6_122$. The maximal dimensions of the alanine racemase (Shaw *et al.*, 1997) and ornithine decarboxylase (Grishin *et al.*, 1999; Kern *et al.*, 1999) dimers, DDC's structural homologs (Grishin *et al.*, 1995), are most consistent with a crystal packing arrangement that includes a screw axis along *c*, as the *c* axis is quite long and the maximal dimensions of the dimers are not adequate to extend that distance. Furthermore, DDC has no large insertions that could span such a distance. In space group $P6_122$, there is one molecule in the asymmetric unit, the calculated solvent content is 43% (Matthews, 1968) and the $R_{\rm merge}$ of data to 2.1 Å is a reasonable 6.8%. A structure analysis is nearly complete in space group $P6_122$.

The authors thank Michelle Momany and Russell Malmburg for the use of their laboratories as well as their advice in the construction of the expression vector. The assistance of John Rose, Zhi-Jie Liu and Bi-Cheng Wang in data collection is gratefully acknowledged. Nandita Bose performed the standardization of the gel-filtration column. Funding support came from a Biotechnology grant to CM and David Chu from the University of Georgia Research Foundation.

References

Abell, L. M. & O'Leary, M. H. (1988). *Biochemistry*, **27**, 5927–5933.
Asada, Y., Tanizawa, K., Nakamura, K., Moriguchi, M. & Soda, K. (1984). *J. Biochem. (Tokyo)*, **95**, 277–282.
Asada, Y., Tanizawa, K., Sawada, S., Suzuki, T., Misono, H. & Soda, K. (1981). *Biochemistry*, **20**, 6881–6886.
Bourot, S., Sire, O., Trautwetter, A., Touze, T., Wu, L. F., Blanco, C. & Bernard, T. (2000). *J. Biol. Chem.* **275**, 1050–1056.
Cohen, G. N. (1985). *Methods Enzymol.* **113**, 596–599.
Girodeau, J. M., Agouridas, C., Masson, M., Pineau, R. & Le Goffic, F. (1986). *J. Med. Chem.* **29**, 1023–1030.
Grishin, N. V., Osterman, A. L., Brooks, H. B., Phillips, M. A. & Goldsmith, E. J. (1999). *Biochemistry*, **38**, 15174–15184.
Grishin, N. V., Osterman, A. L., Goldsmith, E. J. & Phillips, M. A. (1996). *Proteins*, **24**, 272–273.
Grishin, N. V., Phillips, M. A. & Goldsmith, E. J. (1995). *Protein Sci.* **4**, 1291–1304.
Jackson, L. K., Brooks, H. B., Osterman, A. L., Goldsmith, E. J. & Phillips, M. A. (2000). *Biochemistry*, **39**, 11247–11257.
Jancarik, J. & Kim, S.-H. (1991). *J. Appl. Cryst.* **24**, 409–411.
Kern, A. D., Oliveira, M. A., Coffino, P. & Hackert, M. L. (1999). *Structure Fold. Des.* **7**, 567–581.
McPherson, A. (1976). *J. Biol. Chem.* **251**, 6300–6303.
Matthews, B. W. (1968). *J. Mol. Biol.* **33**, 491–497.
Otwinowski, Z. & Minor, W. (1997). *Methods Enzymol.* **276**, 307–326.
Patte, J. (1996). *Escherichia coli and Salmonella: Cellular and Molecular Biology*, edited by F. C. Neidhardt, 2nd ed., pp. 528–541. Washington DC: American Society for Microbiology.
Rosner, A. (1975). *J. Bacteriol.* **121**, 20–28.
Scriven, F., Wlasichuk, K. B. & Palcic, M. M. (1988). *Anal. Biochem.* **170**, 367–371.
Shaw, J. P., Petsko, G. A. & Ringe, D. (1997). *Biochemistry*, **36**, 1329–1342.
Stragier, P., Danos, O. & Patte, J. C. (1983). *J. Mol. Biol.* **168**, 321–331.
Terwilliger, T. C. & Berendzen, J. (1999). *Acta Cryst.* D**55**, 849–861.
White, P. & Kelley, B. (1965). *Biochem. J.* **96**, 75–84.
Work, E. (1957). *Biochem. J.* **91**, 600–610.
Yamada, H. & O'Leary, M. H. (1978). *Biochemistry*, **17**, 669–672.